



CHORUS

This is the accepted manuscript made available via CHORUS. The article has been published as:

Visualizing the radical-pair mechanism of molecular magnetic field effects by magnetic resonance induced electrofluorescence to electrophosphorescence interconversion

Hermann Kraus, Sebastian Bange, Felix Frunder, Ullrich Scherf, Christoph Boehme, and John M. Lupton

Phys. Rev. B **95**, 241201 — Published 14 June 2017

DOI: [10.1103/PhysRevB.95.241201](https://doi.org/10.1103/PhysRevB.95.241201)

Visualizing the radical-pair mechanism of molecular magnetic-field effects by magnetic resonance-induced electrofluorescence to electrophosphorescence interconversion

Hermann Kraus¹, Sebastian Bange¹, Felix Frunder¹, Ullrich Scherf², Christoph Boehme³ and
John M. Lupton^{1,*}

¹Institut für Experimentelle und Angewandte Physik, Universität Regensburg,
Universitätsstrasse 31, 93053 Regensburg, Germany

²Macromolecular Chemistry Group, Chemistry Department and IfP, Bergische Universität
Wuppertal, Gauss-Str. 20, 42097 Wuppertal, Germany

³Department of Physics and Astronomy, University of Utah, Salt Lake City, Utah

*⁾Email: john.lupton@ur.de

We probe the interconversion of spin permutation symmetry of weakly bound electron-hole carrier pairs in an organic light-emitting diode (OLED) by monitoring the changes in yield of recombinant species – singlet and triplet excitons – through fluorescence and phosphorescence, respectively. Spin mixing occurs by spin precession in local hyperfine fields and is suppressed by an external magnetic field, leading to an anticorrelation of fluorescence and phosphorescence yield, which follows the same functionality as magnetoresistance. A resonant radio-frequency field reverses this effect, enhancing spin mixing to raise the phosphorescence and lower the fluorescence. The experiment offers the first direct simultaneous optical probe of the two interconverting spin states in the radical-pair mechanism, which features prominently in models of biological magnetoreception.

Many molecular reactions exhibit strong magnetic-field effects at room temperature with regards to a specific reaction yield¹. A physical picture put forward to explain some of the observations, the radical-pair mechanism², involves the modification by an external magnetic field of the precession of the spins of positive and negative charges in local hyperfine fields. Since such a radical – or electron-hole – pair is Coulombically bound, it can ultimately recombine, with the rate of recombination depending on the spin permutation symmetry of the pair. Many examples of the influence of magnetic fields on reaction yields based on such underlying pair processes have been reported, with measurable magnetic field effects on scales as small as a few microtesla³. Such processes have also been invoked to explain the magnetoceptive abilities of some birds³. While the precise chemical and physiological origin of this ability remains subject to debate, the sensitivity of birds to magnetic fields was recently underlined by the demonstration of an influence of ambient electromagnetic noise on navigational ability⁴. The fact that extremely weak oscillatory fields of nanotesla amplitude⁴ disrupt magnetoception suggests that spin-dependent reaction yields are influenced by very long spin coherence times⁵, possibly of 0.1 millisecond duration⁶. Although much of the research interest in spin-dependent radical-pair processes stems from such biological or model synthetic chemical phenomena, a crucial limitation of investigations is that it is only the reaction yield which is measured rather than the permutation symmetry of the spin pair⁷⁻¹⁰. Analogous spin-pair processes can also arise in the solid state, and have been invoked to explain magnetic resonance phenomena and magnetic-field effects in the conductivity of amorphous silicon¹¹ and molecular organic semiconductor films¹²⁻¹⁸. Such measurements are, in principle, sensitive down to the single-charge level. We recently reported a direct probe of electronic spin coherence in thin films of organic semiconductors incorporated in an OLED configuration by measuring the magnetic-resonance signature in device current¹⁹⁻²¹.

The appeal of OLEDs is that the entire operational principle is based on spin-dependent recombination of injected charges to yield light. Uncorrelated carrier pairs are generated in a spin-statistical ratio of 1:3 singlets to triplets. The two carrier-pair states have different recombination and dissociation rates, so that changes in spin statistics impact the number of free charges and hence conductivity. Time-resolved measurements under magnetic resonance conditions allow the direct quantification of spin-coherence times and reveal the dynamics of hyperfine interactions in the time domain²⁰. Much of the evidence reported to date is consistent with magnetic-field effects and associated magnetic resonance phenomena arising from intermixing between singlet and triplet pair states²². However, device current – like the reaction yield in spin chemistry – is ultimately a secondary integral quantity which reports on changes in spin-pair permutation symmetry without *directly* probing singlet or triplet pair population density. Magnetic resonance has, of course, been probed in organic molecules by monitoring the fluorescence of singlets²¹⁻²³ and the phosphorescence of triplet excited states²⁴⁻²⁶. However, there are no reports of *simultaneous* probing of the two radiative recombination channels which would be required to monitor interconversion between spin species. Here, we demonstrate how to directly probe the density of singlet and triplet pair products in an OLED by monitoring the radiative decay of the molecular excitons formed by pair recombination: phosphorescence from the triplet and fluorescence from the singlet. Anticorrelated changes in the two luminescence channels are observed under an external magnetic field and under magnetic resonance conditions, demonstrating that singlet pairs do indeed convert into triplets and *vice versa*.

Figure 1a) illustrates the dominant electron-hole recombination channels in an OLED. Electrons and holes are injected from opposite electrodes to form bound carrier pairs of singlet or triplet spin configuration. Interconversion between the two species can occur by driving one or both of the carrier spins coherently under magnetic resonance conditions, or

through the spin precession in the local hyperfine fields²⁷. Typically, however, such precession is very slow, so that recombination mostly follows the spin-statistical limit²⁸. The carrier pairs recombine into either singlet or triplet molecular excitons. In pure hydrocarbon compounds, luminescence is dominated by fluorescence from the singlet, with most triplet excitons undergoing non-radiative decay²⁹. In contrast, in organometallic complexes with strong singlet-triplet intersystem crossing in the excited state, radiative recombination from the higher-lying singlet is suppressed so that phosphorescence dominates³⁰⁻³¹. Few materials actually show dual singlet-triplet luminescence, and mostly this can only be identified under time-resolved detection at low temperatures²⁹⁻³². Very few reports of dual luminescence exist for OLEDs³³⁻³⁷. Since we wish to probe small changes in singlet and triplet exciton yield due to magnetic resonance or a static magnetic field, we require a material with strong dual electroluminescence (EL) in which singlet and triplet can be spectrally separated very clearly. A suitable such material is phenylene-substituted ladder-type poly(*para*-phenylene) [PhLPPP, Fig. 1c)] which has a very small (<100ppm) concentration of palladium atoms present in its hydrocarbon framework, left over as catalytic residue^{28,38}. Both triplet and singlet excitons are highly mobile in this material³⁹, which has a high fluorescence quantum yield in the solid state. However, since triplet excitons are longer-lived than singlets, they more readily reach the palladium atoms where intersystem crossing occurs and radiative $T_1 \rightarrow S_0$ recombination becomes possible. In contrast, and unlike conventional organometallic compounds³¹, since the concentration of palladium atoms is so low, excited-state intersystem crossing ($S_1 \rightarrow T_1$) is barely modified⁴⁰. Figure 1b) shows a typical EL spectrum of this material in an OLED of the structure indium-tin oxide/poly(styrene-sulfonate)-doped poly(3,4-ethylenedioxythiophene) (PEDOT:PSS)/PhLPPP/Ba/Al. The device is encapsulated with epoxy and a glass cover slip. Two distinct spectral features are seen: an emission peaking at 460nm, followed by a pronounced vibronic progression, which arises from the singlet exciton transition; and a second feature at 590nm of nearly identical shape from radiative decay of the triplet –

phosphorescence. In pristine material, these two features are clearly separable, and the blue and red areas marked in the figure indicate the spectral regions defined by a dichroic beam splitter and color filters. Following oxidative stress of the material under prolonged device operation, however, a pronounced defect band appears between the fluorescence and phosphorescence at around 550nm^{38,40}. This defect, which arises from the formation of ketones on the ladder-type structure⁴¹, can complicate spectral separation of singlet and triplet, as discussed below.

To provide a magnetic field, the OLED is mounted at the center of a Helmholtz coil and is driven by a Keithley 238 source-measure unit under constant current conditions. EL is collected with an optical fiber in close proximity to the pixel (1×3.17mm² size), passed through a beam splitter, and recorded either on a charge-coupled device spectrometer or, filtered spectrally for singlet and triplet, with two silicon photodiodes coupled to low-noise amplifiers (Femto OE-200-SI). To drive magnetic resonance, the OLED is mounted on the coplanar waveguide structure⁴² shown in panel (d) with the cathode side of the device placed on the waveguide. Radio-frequency (RF) radiation is generated by an HP 83732A high-frequency source and a 20W Mini-Circuits ZHL-20W-13+ amplifier and fed into the waveguide, which is terminated by a 50Ω load. From numerical calculations, we estimate that an RF magnetic field of approximately 100-180μT amplitude is incident on the OLED pixel. The measurement procedure allows for simultaneous recording of magnetoresistance and magnetoEL, with and without an RF field applied. Since the overall sensitivity to changes in EL is of order 90ppm, we can detect EL and resistance in direct current⁴³, without the need of modulation and lock-in procedures, providing truly steady-state measurements and adiabatic field-sweep conditions.

Figure 2 shows two examples of simultaneous magnetoresistance and spectrally resolved magnetoEL, with incident RF fields at frequencies of 560MHz (a) and 400MHz (b). The data result from a single up and down sweep of magnetic field which takes a total of 10 minutes. The magnetoresistance shows an initial increase with magnetic field below 1mT, an effect referred to as the “ultrasmall magnetic-field effect”⁴⁴, and subsequently decreases. A popular model of the magnetoresistance invokes the precession of electron and hole spins in the local hyperfine fields⁴⁵⁻⁴⁶, which leads to mixing between singlet and triplet multiplicity of the carrier pair²⁷. An external magnetic field suppresses this mixing. Various models of this process have been discussed in the literature with regards to OLEDs, and our data appear to follow the established functionalities⁴⁷. A magnetic resonant driving field in turn counteracts this suppression effect by promoting spin mixing, leading to an overall increase of magnetoresistance on resonance, which is clearly seen in both plots. With our dual emitter, the effect of spin mixing in the electron-hole pair exciton precursor state can be visualized directly. An increase in fluorescence with rising magnetic field matches near quantitatively the suppression of phosphorescence. Under magnetic resonance, the effect is partially reversed. This reversal is limited because the resonance line is broader than the driving-field amplitude, which defines the spectral width of the resonant excitation. Charge-carrier spin-resonance line widths are governed by local hyperfine fields, which are determined by the abundant hydrogen. The limitation of the excitation power which can be applied will therefore ultimately limit the size of the subensemble of charge carriers which can be brought into magnetic resonance simultaneously⁴². Nevertheless, the data demonstrate directly that magnetoresistance, and the associated magnetoEL, originates from interconversion between carrier-pair spin species and not, for example, from changes with magnetic field in carrier-pair recombination or dissociation rates²². This relation has previously only been considered for the singlet⁴⁴ or the triplet EL channel⁴⁸ individually, but not in both within one material at the same time. As we discuss below, the fact that in the example in panel (b) the relative static

magnetic-field effect appears slightly weaker in the singlet than in the triplet channel, but the resonance feature is somewhat less pronounced in the triplet, can be attributed to the influence of the parasitic spectral defect band³⁸. This emission is of singlet character but overlaps both singlet and triplet excitonic features and therefore introduces random shunt rates to the detected singlet and triplet transition rates. We stress that both singlet and triplet EL correspond to spin- $\frac{1}{2}$ species, i.e. the individual carrier spins⁴³. This phosphorescence-detected magnetic resonance should not be confused with the spin-1 detection of the triplet exciton resonance, which has been reported previously in molecular emitters but probes spin conversion *within* the triplet manifold rather than singlet-triplet transitions²⁴⁻²⁵. We also note that in our early measurements of magnetoEL on PhLPPP we were not able to resolve these very subtle spectral differences due to limitations in sensitivity²⁸.

The data in Figure 2a) reveal a further subtle feature in the ultralow magnetic-field effect. The inset shows a close-up of the magnetoEL in this region. Singlet and triplet exciton yields follow each other exactly for fields below 1mT before diverging: the ultrasmall magnetic-field effect⁴⁴⁻⁴⁵ with its characteristic *inversion* of field dependency only arises in the resistance and in the singlet channel, but not in the triplet. A similar trend is apparent in panel (b), although with reduced significance due to increased noise. This observation implies that the ultrasmall magnetic-field effect differs fundamentally from the effect on larger magnetic-field scales. This effect has been tentatively attributed to the zero-field splitting of the carrier pair arising from either anisotropic hyperfine interactions⁴⁴ or dipolar spin-spin coupling⁴⁹. The zero-field splitting lifts the degeneracy of the three triplet states and therefore changes mixing rates within the triplet manifold. We propose that this observation could arise from different transition rates of the three triplet states of the carrier pair, which define the triplet symmetry of the exciton – T_+ , T_- or T_0 – to the singlet ground state S_0 . In phosphorescent emitters, the superposition triplet T_0 couples most effectively to the superposition state S_0 .

The yield of this superposition triplet species therefore appears to not be affected by the field on very small magnetic-field scales of order the zero-field splitting of the carrier pairs.

Finally, we demonstrate the data quality achievable by employing lock-in detection to study the resonance spectra more closely, demodulating against a square-wave full amplitude modulation of the RF source at 23Hz. Figure 3a) shows spectra measured at three different frequencies. All resonances are accurately described by the superposition of two Gaussians with standard deviations of 0.38mT and 0.72mT. These two Gaussians correspond to the hyperfine-field distributions experienced by the electron and hole spins^{21,43} and are shown in green in the right-most singlet resonance curve for illustration purposes. However, in a perfect pair process, the areas of both Gaussian peaks must be identical, since resonant excitation of electron and hole each map onto the same observable of differential current or EL²¹. This is not the case here, and evidently even the overall singlet and triplet resonance peaks have different areas. This discrepancy arises because of the fact that a spectrally broad defect band is always superimposed on the narrow singlet and triplet EL peaks and cannot be separated fully by spectral filtering³⁸. The influence of this feature depends on material quality and device age. Figure 3b) plots the change with time of the differential EL signal on resonance for singlet and triplet spectral features. Only at the outset of the measurement do singlet and triplet actually have the opposite resonance signs. After two hours of continuous operation, the signal associated with the phosphorescence resonance vanishes entirely for a short time before both resonance features become negative. The amplitude of the resonance from the red part of the spectrum, the superposition of phosphorescence and keto defect, changes faster with time than the blue part of the spectrum, the superposition of singlet fluorescence and defect emission. The inversion of resonance sign with prolonged device operation time arises because the contribution of the broad keto-defect emission band to the EL spectrum increases with time and the defect itself acts as a charge-carrier trap⁵⁰ with a distinct magnetic-field

sensitivity⁵¹. This observation of an inversion of resonance amplitude with time contains further information on material-specific recombination kinetics: it demonstrates that the broad keto-defect band has singlet character rather than mirroring the pure triplet species. This is an interesting conclusion since delayed luminescence experiments have demonstrated that triplet excitons can feed into the defect band, which is common to many polycyclic aromatic hydrocarbons, on timescales of seconds³². The keto defect can therefore harvest long-lived triplet excitons³², but when carriers recombine directly on the defect it acts as a pure singlet fluorophore.

OLEDs offer highly sensitive and versatile conditions to probe spin-dependent recombination processes and their sensitive responses to magnetic fields. The experiments presented here were carried out under d.c. OLED operation conditions and time-averaged photodetection. With gated luminescence detection we expect to be able to separate fluorescence and phosphorescence signatures even more clearly. In combination with pulsed magnetic resonance excitation²⁰ it should be possible to directly probe, in the time domain, coherent singlet-triplet interconversion in the change in OLED luminescence color. Such experiments would constitute alternatives to conventional singlet-triplet qubit systems based on coupled quantum dots⁵²⁻⁵⁴ which are considered as building blocks for quantum information processing architectures.

The authors are indebted to Dr. Kipp van Schooten and Dr. Hans Malissa for helpful discussions and to the DFG for funding through SFB 679. CB acknowledges support through the US Department of Energy, Office of Basic Energy Sciences, Division of Materials Sciences and Engineering under Award #DESC0000909.

References

- [1] U. E. Steiner and T. Ulrich, *Chem. Rev.* **89**, 51 (1989).
- [2] T. Ritz, S. Adem, and K. Schulten, *Biophys. J.* **78**, 707 (2000).
- [3] K. Maeda, K. B. Henbest, F. Cintolesi, I. Kuprov, C. T. Rodgers, P. A. Liddell, D. Gust, C. R. Timmel, and P. J. Hore, *Nature* **453**, 387 (2008).
- [4] S. Engels *et al.*, *Nature* **509**, 353 (2014).
- [5] J. M. Cai and M. B. Plenio, *Phys. Rev. Lett.* **111**, 230503 (2013).
- [6] E. M. Gauger, E. Rieper, J. J. L. Morton, S. C. Benjamin, and V. Vedral, *Phys. Rev. Lett.* **106**, 040503, 040503 (2011).
- [7] C. A. Dodson, C. J. Wedge, M. Murakami, K. Maeda, M. I. Wallace, and P. J. Hore, *Chem. Commun.* **51**, 8023 (2015).
- [8] J. R. Woodward, C. R. Timmel, K. A. McLauchlan, and P. J. Hore, *Phys. Rev. Lett.* **87**, 077602 (2001).
- [9] K. B. Henbest, P. Kukura, C. T. Rodgers, P. J. Hore, and C. R. Timmel, *J. Am. Chem. Soc.* **126**, 8102 (2004).
- [10] T. Ritz, P. Thalau, J. B. Phillips, R. Wiltschko, and W. Wiltschko, *Nature* **429**, 177 (2004).
- [11] D. Kaplan, I. Solomon, and N. F. Mott, *J. Phys. Lett.* **39**, L51 (1978).
- [12] E. L. Frankevich, I. A. Sokolik, D. I. Kadyrov, and V. M. Kobryanskii, *JETP Lett.* **36**, 486 (1982).
- [13] V. Dyakonov, G. Rosler, M. Schwoerer, and E. L. Frankevich, *Phys. Rev. B* **56**, 3852 (1997).
- [14] K. Morgan and R. Pethig, *Nature* **213**, 900 (1967).
- [15] P. Desai, P. Shakya, T. Kreouzis, W. P. Gillin, N. A. Morley, and M. R. J. Gibbs, *Phys. Rev. B* **75**, 094423 (2007).

- [16] T. L. Francis, O. Mermer, G. Veeraraghavan, and M. Wohlgenannt, *New J. Phys.* **6**, 185 (2004).
- [17] J. Kalinowski, M. Cocchi, D. Virgili, P. Di Marco, and V. Fattori, *Chem. Phys. Lett.* **380**, 710 (2003).
- [18] J. M. Lupton and C. Boehme, *Nat. Mater.* **7**, 598 (2008).
- [19] W. J. Baker, T. L. Keevers, J. M. Lupton, D. R. McCamey, and C. Boehme, *Phys. Rev. Lett.* **108**, 267601 (2012).
- [20] H. Malissa, M. Kavand, D. P. Waters, K. J. van Schooten, P. L. Burn, Z. V. Vardeny, B. Saam, J. M. Lupton, and C. Boehme, *Science* **345**, 1487 (2014).
- [21] M. Kavand, D. Baird, K. van Schooten, H. Malissa, J. M. Lupton, and C. Boehme, *Phys. Rev. B* **94**, 075209 (2016).
- [22] S. P. Kersten, A. J. Schellekens, B. Koopmans, and P. A. Bobbert, *Phys. Rev. Lett.* **106**, 197402 (2011).
- [23] L. S. Swanson, J. Shinar, A. R. Brown, D. D. C. Bradley, R. H. Friend, P. L. Burn, A. Kraft, and A. B. Holmes, *Phys. Rev. B* **46**, 15072 (1992).
- [24] D. A. Antheunis, J. Schmidt, and J. H. Van der Waals, *Chem. Phys. Lett.* **6**, 255 (1970).
- [25] J. Schmidt, W. G. Van Dorp, and J. H. Van der Waals, *Chem. Phys. Lett.* **8**, 345 (1971).
- [26] G. Li, J. Shinar, and G. E. Jabbour, *Phys. Rev. B* **71**, 235211 (2005).
- [27] R. C. Roundy and M. E. Raikh, *Phys. Rev. B* **88**, 125206 (2013).
- [28] M. Reufer, M. J. Walter, P. G. Lagoudakis, B. Hummel, J. S. Kolb, H. G. Roskos, U. Scherf, and J. M. Lupton, *Nat. Mater.* **4**, 340 (2005).
- [29] A. Köhler, J. S. Wilson, and R. H. Friend, *Adv. Eng. Mater.* **4**, 453 (2002).
- [30] M. A. Baldo, D. F. O'Brien, Y. You, A. Shoustikov, S. Sibley, M. E. Thompson, and S. R. Forrest, *Nature* **395**, 151 (1998).

- [31] S. Haneder *et al.*, *Adv. Mater.* **20**, 3325 (2008).
- [32] D. Chaudhuri, H. Wettach, K. J. van Schooten, S. Liu, E. Sigmund, S. Höger, and J. M. Lupton, *Angew. Chem. Int. Ed.* **49**, 7714 (2010).
- [33] S. Hoshino and H. Suzuki, *Appl. Phys. Lett.* **69**, 224 (1996).
- [34] C. Garditz, A. G. Muckl, and M. Cölle, *J. Appl. Phys.* **98**, 104507 (2005).
- [35] D. Chaudhuri *et al.*, *Angew. Chem. Int. Ed.* **52**, 13449 (2013).
- [36] W. Ratzke *et al.*, *J. Phys. Chem. Lett.* **7**, 4802 (2016).
- [37] J. M. Lupton and J. Klein, *Chem. Phys. Lett.* **363**, 204 (2002).
- [38] J. M. Lupton, A. Pogantsch, T. Piok, E. J. W. List, S. Patil, and U. Scherf, *Phys. Rev. Lett.* **89**, 167401 (2002).
- [39] M. Reufer, P. G. Lagoudakis, M. J. Walter, J. M. Lupton, J. Feldmann, and U. Scherf, *Phys. Rev. B* **74**, 241201 (2006).
- [40] S. Bange, U. Scherf, and J. M. Lupton, *J. Am. Chem. Soc.* **134**, 1946 (2012).
- [41] L. Romaner, G. Heimel, H. Wiesenhofer, P. Scandiucci de Freitas, U. Scherf, J.-L. Brédas, E. Zojer, E. J. W. List, *Chem. Mater.* **16**, 4667 (2004).
- [42] W. J. Baker, K. Ambal, D. P. Waters, R. Baarda, H. Morishita, K. van Schooten, D. R. McCamey, J. M. Lupton, and C. Boehme, *Nat. Commun.* **3**, 898 (2012).
- [43] D. P. Waters, G. Joshi, M. Kavand, M. E. Limes, H. Malissa, P. L. Burn, J. M. Lupton, and C. Boehme, *Nature Phys.* **11**, 910 (2015).
- [44] T. D. Nguyen, B. R. Gautam, E. Ehrenfreund, and Z. V. Vardeny, *Phys. Rev. Lett.* **105**, 166804 (2010).
- [45] T. D. Nguyen, G. Hukic-Markosian, F. J. Wang, L. Wojcik, X. G. Li, E. Ehrenfreund, and Z. V. Vardeny, *Nat. Mater.* **9**, 345 (2010).
- [46] Y. Sheng, T. D. Nguyen, G. Veeraraghavan, O. Mermer, M. Wohlgenannt, S. Qiu, and U. Scherf, *Phys. Rev. B* **74**, 045213 (2006).

- [47] A. Schellekens, W. Wagemans, S. Kersten, P. Bobbert, and B. Koopmans, *Phys. Rev. B* **84**, 075204 (2011).
- [48] K. Xu, D. Z. Yang, Y. B. Zhao, J. S. Chen, and D. G. Ma, *Org. Electron.* **15**, 590 (2014).
- [49] K. J. van Schooten, D. L. Baird, M. E. Limes, J. M. Lupton, and C. Boehme, *Nat. Commun.* **6**, 6688 (2015).
- [50] J. M. Lupton and J. Klein, *Phys. Rev. B* **65**, 193202 (2002).
- [51] M. Cox, M. H. A. Wijnen, G. A. H. Wetzelaer, M. Kemerink, P. W. M. Blom, and B. Koopmans, *Phys. Rev. B* **90**, 155205 (2014).
- [52] J. R. Petta, A. C. Johnson, J. M. Taylor, E. A. Laird, A. Yacoby, M. D. Lukin, C. M. Marcus, M. P. Hanson, and A. C. Gossard, *Science* **309**, 2180 (2005).
- [53] F. H. L. Koppens *et al.*, *Science* **309**, 1346 (2005).
- [54] B. M. Maune *et al.*, *Nature* **481**, 344 (2012).

Figure captions.

Figure 1. Spectrally resolved optically detected magnetic resonance of a dual singlet-triplet emitting OLED. a) Free injected charge carriers in the OLED attract Coulombically to form weakly coupled spin pairs. The overall spin permutation symmetry of the pair can oscillate between singlet and triplet configuration by either spin precession in the local hyperfine fields or by coherent driving in an external magnetically resonant radio-frequency driving field. Ultimately, the carrier pairs either dissociate again or recombine to form tightly bound molecular singlet or triplet exciton species. Singlets decay by fluorescence and triplets by phosphorescence. b) Electroluminescence (EL) spectrum of an OLED made of phenylene-substituted ladder-type poly(*para*-phenylene) (PhLPPP), the structure of which is shown in c). The EL is characterized by distinct fluorescence (singlet) and phosphorescence (triplet) features, which are separated spectrally by a combination of dichroic beam splitters and filters. The spectral regions defined by the setup are indicated. d) Illustration of the copper coplanar waveguide structure used for magnetic resonant excitation of the OLED charge carrier states. The dimensions of the waveguide are $h=1.6\text{mm}$, $t=35\mu\text{m}$, $s=0.5\text{mm}$, $w=4\text{mm}$, with the FR-4 circuit-board substrate dielectric $\epsilon_s=4.5$.

Figure 2. Spectrally resolved steady-state magnetoEL and magnetoresistance under magnetic resonant excitation of charge carriers. Data points show the average of up and down sweeps in magnetic field. a) The magnetoresistance correlates directly with an increase in fluorescence and a decrease in phosphorescence, which is reversed under magnetic resonance at 20mT (560MHz). The inset shows the region of the ultraslow magnetic-field effect below 1mT. In this region, singlet and triplet yield follow exactly the same functionality, with the increase in magnetoresistance correlating with a decrease in luminescence. Individual measurement data points are shown enlarged for clarity. b) A second OLED device with the resonance feature at

14.3mT (400MHz). In this example a weak EL contribution from the keto defect limits the quantitative match between singlet enhancement and triplet quenching.

Figure 3. Fluorescence and phosphorescence magnetic resonance features measured under lock-in detection to remove the steady-state magnetoEL background. a) The resonance curves are described by the same sum of two Gaussians with standard deviations of 0.38 and 0.72mT, indicated by the dashed green lines. The resonance amplitudes of singlet and triplet do not match perfectly because a third luminescence species, the broad keto-defect emission band³⁸, contributes to EL after prolonged device operation. This defect band leads to a sign inversion of the phosphorescence resonance (red squares) with time, as plotted in (b).

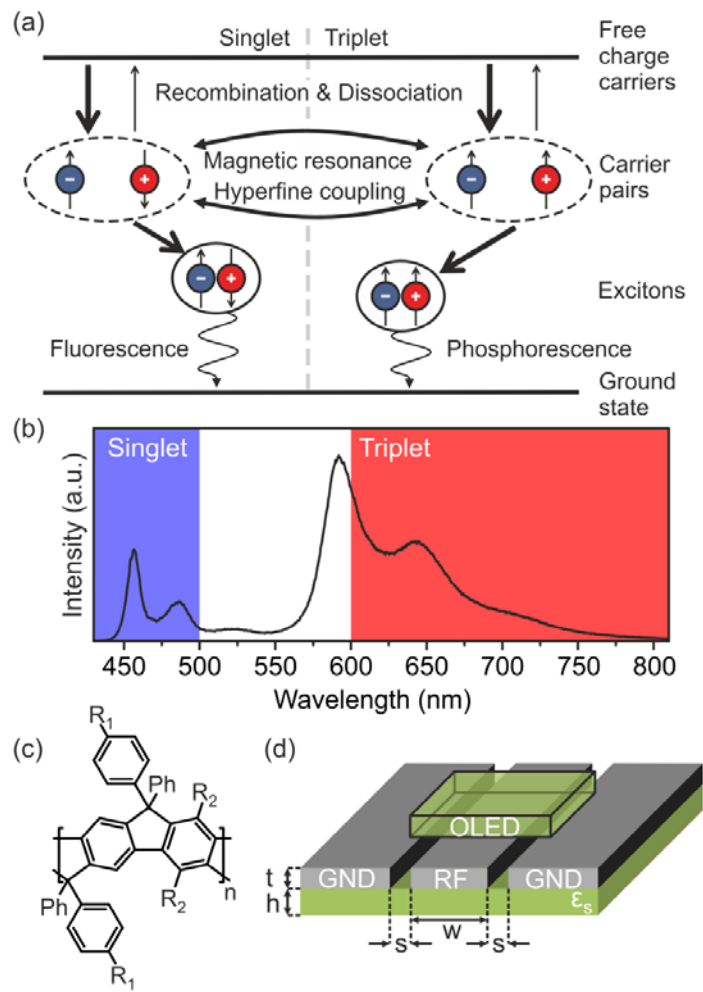


Figure 1.

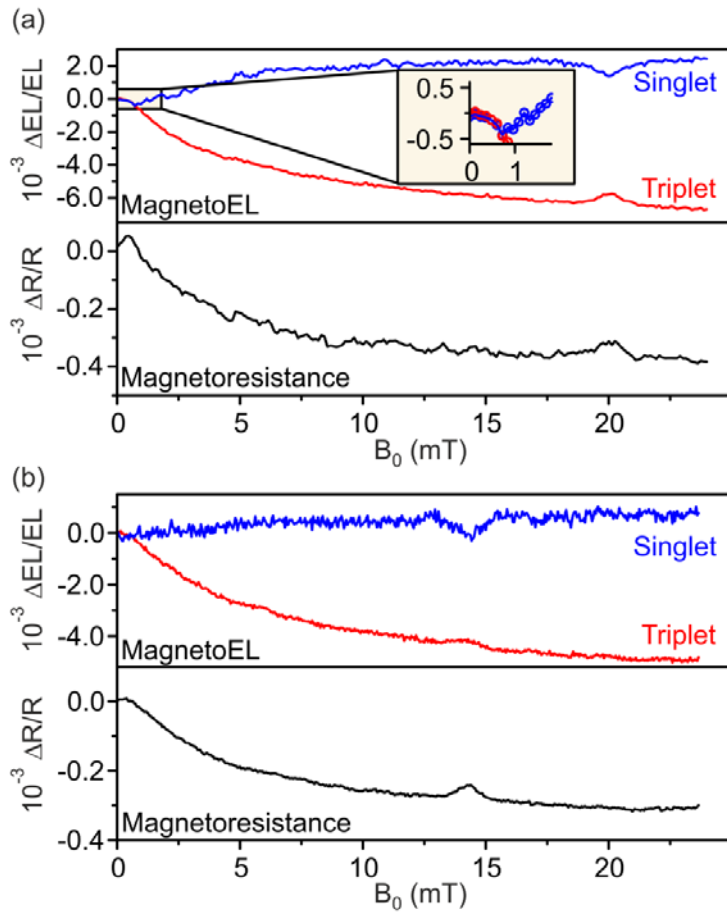


Figure 2.

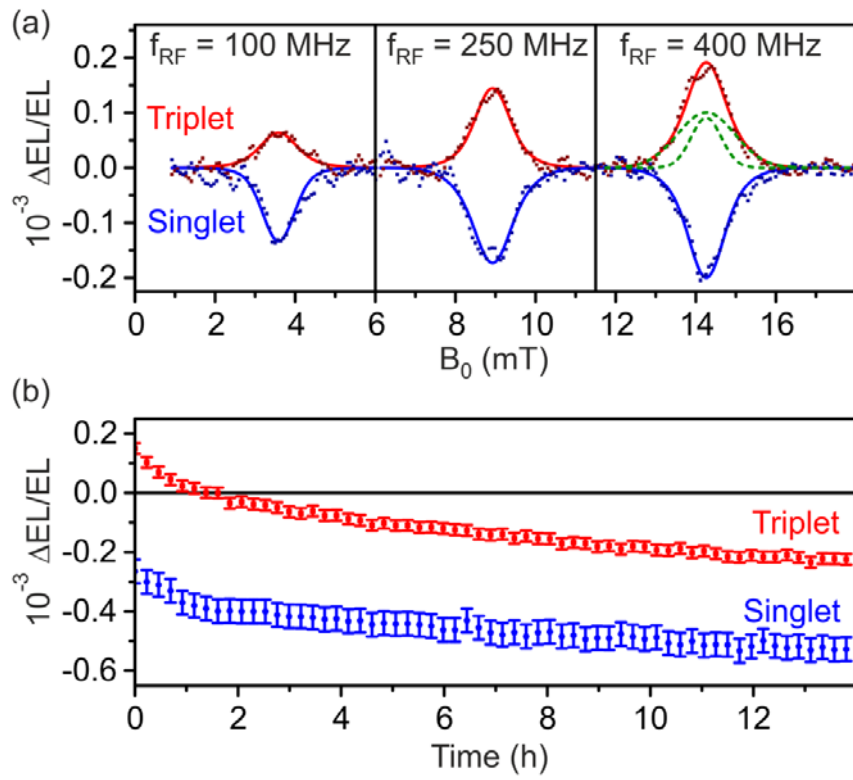


Figure 3.